Relativistic treatment of spin-transfer observables in quasielastic $(\vec{p},\vec{n})$ scattering

C.J. Horowitz
Nuclear Theory Center and Department of Physics, Indiana University, Bloomington, Indiana 47505

J. Piekarewicz
Supercomputer Computations Research Institute, Florida State University, Tallahassee, Florida 32306
(Received 1 July 1994)

We calculate all spin-transfer observables for the quasielastic $(\vec{p},\vec{n})$ reaction in a relativistic plane-wave impulse approximation. The nuclear structure information is contained in a large set of nuclear response functions that are computed in nuclear matter using a relativistic random-phase approximation to the Walecka model. A reduced value of the nucleon mass in the medium induces important dynamical changes in the residual isovector interaction relative to its nonrelativistic counterpart. As a result, good agreement is found for all spin observables – including the spin-longitudinal to spin-transverse ratio – when compared to the original ($q = 1.72$ fm^{-1}) NTOF (neutron time-of-flight facility) experiment. In contrast, the spin-longitudinal to spin-transverse ratio is underpredicted at $q = 1.2$ fm^{-1} and overpredicted at $q = 2.5$ fm^{-1}. We comment on the role of distortions as a possible solution to this discrepancy.

PACS number(s): 25.40.Kv, 24.10.Jv, 21.60.Jz

I. INTRODUCTION

The prominence of the pion as a mediator of the nucleon-nucleon (NN) force is indisputable. Yet, its propagation through the nuclear medium is far from understood and remains the source of considerable debate. The propagation of a pion through the nuclear medium is modified by its coupling to nuclear (e.g., particle-hole) excitations. This information is contained in the meson self-energy whose imaginary part is a physical observable characterizing the linear response of the system to an external probe. Hence, information about pion propagation through the nuclear medium may be obtained, in principle, from a measurement of the nuclear isovector response. Several different experiments have been designed with the aim of extracting the nuclear isovector response [1,2], yet the development of sophisticated experimental facilities and techniques have made the $(\vec{p},\vec{n})$ reaction the paradigm [3,4]. Indeed, the recent availability of a complete set of $(\vec{p},\vec{n})$ spin-transfer observables has made possible the extraction of the spin-longitudinal response (R_L). This response is important because it is sensitive to the propagation of the pion through the nuclear medium. Moreover, it is not accessible with electromagnetic probes, yet it is as fundamental as the longitudinal and transverse responses measured in electron scattering.

Inextricably linked to the pion in the study of the isovector response is the ρ meson. Although the heavier ρ meson contributes to the more uncertain short-distance dynamics, its role as a mediator of the NN interaction is fairly well established. Indeed, meson-exchange models of the NN interaction, as well as the large isovector anomalous moment of the nucleon, suggest a strong tensor coupling of the nucleon to the ρ. This tensor-coupling is, in particular, responsible for the regularization of the large pionic contribution to the NN tensor force. Moreover, rho exchange dominates the spin-transverse component of the isovector interaction and is, thus, ultimately responsible for the collective behavior of the spin-transverse response (R_T). This is in contrast to R_L which is dominated by pion exchange.

The $\pi - \rho$ mass difference makes the study of the momentum-transfer dependence of R_L and R_T particularly interesting. In the conventional $(\pi + \rho + g')$ model of the residual interaction the longitudinal component of the interaction becomes attractive at a momentum transfer of $q \simeq 1$ fm^{-1} due to the small pion mass. In contrast, the larger mass of the ρ meson causes the transverse component to remain repulsive well beyond $q \simeq 2.5$ fm^{-1}. This behavior led Alberico, Ericson, and Molinari to predict a softening and enhancement of the spin-longitudinal response and a quenching and hardening of the spin-transverse response [5]. Thus, they suggested that a measurement of R_L and R_T should reveal a large enhancement in the ratio (R_L/R_T) at low-energy loss relative to its free Fermi-gas value. The lack of an experimental enhancement in R_L/R_T constitutes one of the most serious challenges facing nuclear physics today [1–4].

The measurement of $(\vec{p},\vec{n})$ spin observables in the quasielastic region might constitute the cleanest and most unambiguous way of probing the nuclear spin-isospin response. First, the reactive content of the reaction is dominated by quasifree nucleon knockout. Indeed, for momentum transfers in excess of 1 fm^{-1} a clear quasielastic peak is seen at an excitation energy close to the corresponding one for free NN scattering. Moreover, free NN spin observables provide a base line, against which possible medium effects may be inferred. Deviations of spin observables from their free NN values are likely to arise from a modification of the NN interaction inside the nuclear medium or from a change in the collective response of the target. Indeed, relativistic calculations predict medium modifications to the free NN interaction stemming from an enhanced lower

component of Dirac spinors in the medium. This modified NN interaction is responsible for one of the clearest relativistic signatures found to date — the quenching of the analyzing power in $(\vec{p},\vec{p}')$ quasielastic scattering [6]. Second, nonrelativistic calculations of $(\vec{p},\vec{n})$ observables at $q = 1.72$ fm^{-1} have shown that while distortions provide an overall reduction of the cross section, they do so without substantially modifying the distribution of strength [7]. Finally, the $(\vec{p},\vec{n})$ reaction acts as an isospin filter by isolating the isovector component of the response. Thus, a combined measurement of $(\vec{p},\vec{n})$ and $(\vec{p},\vec{p}')$ spin observables should enable one to determine the spin-isospin content of the nuclear response.

Recently we have reported the first relativistic calculations of R_L/R_T using a relativistic random-phase approximation (RPA) to the Walecka model [8]. In the Walecka model nucleons interact via the exchange of isoscalar σ (scalar) and ω (vector) mesons [9,10]. In a mean-field approximation the scalar and vector meson fields are replaced by their classical expectation value. The mean-field approximation is characterized by the appearance of strong scalar and vector mean fields which induce large shifts in the mass and energy of a particle in the medium. Isoscalar effects from a reduced nucleon mass lead to important changes in the isovector response. In particular, a reduced nucleon mass is responsible for a shift in the position and an increase in the width of the quasielastic peak that are sufficient to explain the "quenching" and "hardening" of the transverse response. In addition, a smaller nucleon mass leads to a significant reduction in the effective $NN\pi$ coupling in the nuclear medium [11]. This effect reduces the enhancement of the spin-longitudinal response relative to nonrelativistic predictions and leads to no enhancement in R_L/R_T, in agreement with experiment [3,4]. In this work we present a detailed account of our assumptions and calculational scheme. Moreover, we extend previous results, limited to R_L/R_T, to include all spin-transfer observables.

We have organized our paper as follows: In Sec. II we present the relevant formalism for the calculation of the isovector response. This section includes a discussion of the different assumptions and approximations leading to the spin-dependent cross section. The relativistic parametrization of the underlying NN t matrix, the nuclear isovector response, and the residual particle-hole interaction are also presented in this section. In Sec. III results are presented for a variety of approximations ranging from a free Fermi gas to a relativistic RPA treatment of the nuclear response. Finally, Sec. IV contains a summary of our findings and conclusions.

II. FORMALISM

A. Relativistic plane-wave impulse approximation

In the impulse approximation the interaction between two nucleons in the medium is assumed to be identical to their interaction in free space. Thus, in the impulse approximation the in-medium NN interaction is fully determined from two-nucleon data. A convenient representation of the NN amplitude is given in terms of five Lorentz-invariant amplitudes. A standard parametrization of the NN amplitude includes scalar, vector, tensor, pseudoscalar, and axial-vector amplitudes [12]

$$\mathcal{F} = \mathcal{F}_S + \mathcal{F}_V \gamma^{\mu}_{(1)}\gamma_{\mu(2)} + \mathcal{F}_T \sigma^{\mu\nu}_{(1)}\sigma_{\mu\nu(2)} + \mathcal{F}_P \gamma^5_{(1)}\gamma^5_{(2)} + \mathcal{F}_A \gamma^{\mu}_{(1)}\gamma^5_{(1)}\gamma_{\mu(2)}\gamma^5_{(2)} , \quad (1)$$

where the subscripts (1) and (2) refer to the incident and struck nucleons, respectively, and we will adopt the conventions of Bjorken and Drell for the gamma matrices [13]. Note that the amplitudes depend on two Lorentz-invariant quantities: the square of the total four momentum (s) and the square of the four-momentum transfer (t). Matrix elements of $\mathcal{F}$ taken between free Dirac spinors can be regarded as known since they are directly related to the free NN phase shifts [12].

In the following presentation of the $(\vec{p},\vec{n})$ cross section we shall use only the scalar invariant, for simplicity. Our final results, presented at the end of this section, will include all additional Lorentz structures. In a relativistic plane-wave impulse approximation (RPWIA) the cross section for the charge-exchange process is given by

$$d\sigma_{\mathbf{s's}} = \frac{2\pi}{|\mathbf{v}|}\int \frac{d\mathbf{p}'}{(2\pi)^3}|t_S|^2 L(\mathbf{p}s;\mathbf{p}'s')S(\mathbf{q},\omega) , \quad (2)$$

where $|\mathbf{v}|$ is the incident flux in the rest frame of the nucleus, $\mathbf{p}$ ($\mathbf{p}'$) and s (s') are the momentum and spin projection of the initial (final) nucleon, and $\mathbf{q}$ and ω are the momentum and energy transfer to the nucleus, respectively. All dynamical information about the process is contained in the three quantities t_S, L, and S. t_S is the scalar component of the NN t matrix driving the reaction. The plane-wave tensor $L(\mathbf{p}s;\mathbf{p}'s')$ contains information about the polarization of the incoming and outgoing nucleon. Finally, $S(\mathbf{q},\omega)$ characterizes the nuclear response. We address each contribution individually below.

The scalar component of the NN t matrix in the center of momentum frame is simply related to the corresponding Lorentz invariant amplitude [6]

$$t_S \equiv -8\pi i \frac{p_{\rm c.m.}E_{\rm c.m.}}{M^2}\mathcal{F}_S . \quad (3)$$

In particular, in a one-boson exchange description of the scattering process, and to lowest order in the coupling, it reduces to

$$t_S \to v_S = \frac{g_S^2}{q_\mu^2 - m_S^2} , \quad (4)$$

where q_μ is the (spacelike) four-momentum transfer to the nucleus, and m_S and g_S are the scalar mass and coupling constant, respectively.

The polarization information is contained in the projectile "tensor"

$$L(\mathbf{p},\mathbf{s};\mathbf{p}',\mathbf{s}') = |\,\bar{u}(\mathbf{p}',s')\,\mathbf{1}\,u(\mathbf{p},s)|^2 . \quad (5)$$

In a relativistic plane-wave approximation the tensor can

be written exclusively in terms of free Dirac spinors. In nuclear matter, however, the effective mass of a nucleon is reduced relative to its free space value by the presence of a scalar mean field. Thus, for a nucleon propagating through nuclear matter the in-medium Dirac spinor becomes [10]

$$\mathcal{U}(\mathbf{p},s)=\sqrt{\frac{E^\star_{\mathbf{p}}+M^\star_p}{2E^\star_{\mathbf{p}}}}\begin{pmatrix}1\\ \dfrac{\sigma\cdot\mathbf{p}}{E^\star_{\mathbf{p}}+M^\star_p}\end{pmatrix}\chi_s\ , \tag{6}$$

where $M^\star_p$ is the effective mass of the projectile and the on-shell energy is given by

$$E^\star_{\mathbf{p}}=\sqrt{\mathbf{p}^2+M^{\star 2}_p}\ . \tag{7}$$

Note that the normalization implied by Eq. (6) differs from the one in Ref. [13] in that

$$\mathcal{U}^\dagger(\mathbf{p},s)\,\mathcal{U}(\mathbf{p},s')=\delta_{ss'}\ . \tag{8}$$

The plane-wave approximation enables one to write, and ultimately to evaluate, the projectile tensor using Feynman's trace techniques

$$L(\mathbf{p},\mathbf{s};\mathbf{p}',\mathbf{s}')=\mathrm{Tr}\left[\left(\frac{\not p+M^\star_p}{2E^\star_{\mathbf{p}}}\right)\left(\frac{1+\gamma^5\not s}{2}\right)\left(\frac{\not p'+M^\star_p}{2E^\star_{\mathbf{p}'}}\right)\times\left(\frac{1+\gamma^5\not s'}{2}\right)\right]\ . \tag{9}$$

Here $p^\mu(p'^\mu)$ and $s^\mu(s'^\mu)$ are the four-momentum and four-spin of the incoming(outgoing) nucleon, respectively. Note that they satisfy the following relations:

$$p^\mu p_\mu=p'^\mu p'_\mu=M^{\star 2}_p\ ;\quad s^\mu s_\mu=s'^\mu s'_\mu=-1\ ;\quad p^\mu s_\mu=p'^\mu s'_\mu=0\ . \tag{10}$$

The nuclear-structure information is contained in the scalar response function

$$S(\mathbf{q},\omega)=\sum_n|\langle\Psi_n|\hat\rho_S(\mathbf{q})|\Psi_0\rangle|^2\,\delta(\omega-\omega_n)\ . \tag{11}$$

The scalar density

$$\hat\rho_S(\mathbf{q})\equiv\int d\mathbf{x}e^{i\mathbf{q}\cdot\mathbf{x}}\bar\psi(\mathbf{x})\psi(\mathbf{x}) \tag{12}$$

is responsible for inducing transitions between the exact nuclear ground state (Ψ_0) and an excited state (Ψ_n) with excitation energy $\omega_n=(E_n-E_0)$. Specific details about the calculation of the response are postponed until the next section.

The evaluation of the phase-space and incoming flux factors is the only task that remains to be performed. The phase-space factor is related to the experimentally detected energy $\left(E'=\sqrt{\mathbf{p}'^2+M^2}\right)$ of the outgoing proton

$$\int\frac{d\mathbf{p}'}{(2\pi)^3}=\int\frac{|\mathbf{p}'|E'}{(2\pi)^3}d\Omega\,dE'\ . \tag{13}$$

The incident flux factor, on the other hand, is evaluated in nuclear matter for an incoming nucleon having an effective mass $M^\star_p$

$$|\mathbf{v}|=\frac{|\mathbf{p}|}{E^\star_{\mathbf{p}}}\ . \tag{14}$$

Collecting all appropriate terms leads to the following expression for the RPWIA spin-dependent cross section:

$$\frac{d^2\sigma_{\mathbf{s}'\mathbf{s}}}{d\Omega dE'}=\frac{2\pi}{(|\mathbf{p}|/E^\star_{\mathbf{p}})}\frac{|\mathbf{p}'|E'}{(2\pi)^3}|t_S|^2L(\mathbf{p},\mathbf{s};\mathbf{p}',\mathbf{s}')S(\mathbf{q},\omega)\ . \tag{15}$$

The evaluation of the cross section gets substantially more complicated when all Lorentz structures of the NN amplitude are incorporated. The structure of the cross section, however, remains unchanged:

$$\frac{d^2\sigma_{\mathbf{s}'\mathbf{s}}}{d\Omega dE'}=\frac{2\pi}{(|\mathbf{p}|/E^\star_{\mathbf{p}})}\frac{|\mathbf{p}'|E'}{(2\pi)^3}\sum_{\alpha\beta}t_\alpha t^*_\beta L^{\alpha\beta}(\mathbf{p},\mathbf{s};\mathbf{p}',\mathbf{s}')S_{\alpha\beta}(\mathbf{q},\omega)\quad(\alpha,\beta=S,V,T,P,A)\ . \tag{16}$$

The main complication arises due to the mixing of the many different Lorentz structures of the NN interaction. This mixing, however, is already familiar from electron-scattering calculations. Indeed, in electron scattering one must compute various nuclear response functions (e.g., mixed vector-tensor response) due to the anomalous moment of the nucleon. In the present case the nuclear structure information is contained in a large set of nuclear response functions

$$S_{\alpha\beta}(\mathbf{q},\omega)=\sum_n\langle\Psi_n|\hat J_\alpha(\mathbf{q})|\Psi_0\rangle\langle\Psi_n|\hat J_\beta(\mathbf{q})|\Psi_0\rangle^*\times\delta(\omega-\omega_n)\ , \tag{17}$$

which are expressed in terms of nuclear currents containing all possible Lorentz structures

$$\hat J^\alpha(\mathbf{q})\equiv\int d\mathbf{x}e^{i\mathbf{q}\cdot\mathbf{x}}\bar\psi(\mathbf{x})\lambda^\alpha\psi(\mathbf{x})\ . \tag{18}$$

Note that we have introduced the following definitions:

$$\lambda^\alpha\equiv\left\{1,\gamma^\mu,\sigma^{\mu\nu},i\gamma^5,\gamma^\mu\gamma^5\right\}\ ;\quad\bar{\lambda^\alpha}\equiv\gamma^0\lambda^{\alpha\dagger}\gamma^0=\lambda^\alpha\ . \tag{19}$$

Likewise, the projectile tensor has been suitably generalized from Eq. (9) to

$$L^{\alpha\beta}(\mathbf{p},\mathbf{s};\mathbf{p}',\mathbf{s}')=\mathrm{Tr}\left[\lambda^\alpha\left(\frac{\not p+M^\star_p}{2E^\star_{\mathbf{p}}}\right)\left(\frac{1+\gamma^5\not s}{2}\right)\lambda^\beta\times\left(\frac{\not p'+M^\star_p}{2E^\star_{\mathbf{p}'}}\right)\left(\frac{1+\gamma^5\not s'}{2}\right)\right]\ . \tag{20}$$

B. Nuclear response functions

An essential component of the calculation of the cross section is the nuclear response (as before, we present the relevant ideas by considering only the scalar response, for simplicity). The nuclear response can be related, in a model-independent way, to the imaginary part of the scalar polarization [14]

$$\begin{aligned} S(\mathbf{q},\omega) &= \sum_n \left| \langle \Psi_n | \hat{\rho}_S(\mathbf{q}) | \Psi_0 \rangle \right|^2 \delta(\omega - \omega_n) \\ &= -\frac{1}{\pi} \mathcal{I}_{\rm m} \sum_n \frac{\langle \Psi_0 | \hat{\rho}_S(-\mathbf{q}) | \Psi_n \rangle \langle \Psi_n | \hat{\rho}_S(\mathbf{q}) | \Psi_0 \rangle}{\omega - \omega_n + i\eta} \\ &\equiv -\frac{1}{\pi} \mathcal{I}_{\rm m} \Pi_S(\mathbf{q},\omega) \ . \end{aligned} \tag{21}$$

This identification is useful because it will enable us to extend the calculation beyond the single-particle (or uncorrelated) response. Indeed, we will compute all spin-transfer observables by, first, calculating the single-particle response of a relativistic mean-field ground state and, then, will incorporate long-range correlations by solving for the polarization in a relativistic random-phase approximation (RPA). All nuclear response functions will be calculated in infinite nuclear matter. This is an additional and important approximation of the model.

In a mean-field approximation to the nuclear-matter ground state, the scalar polarization can be evaluated readily using Wick's theorem

$$i\Pi_S(q) = \int \frac{d^4k}{(2\pi)^4} {\rm Tr}[G(k+q)G(k)] \ . \tag{22}$$

Here $G(k)$ is the self-consistent nucleon propagator [10]

$$\begin{aligned} G(k) = \left(\not{\bar{k}} + M_t^\star \right) \Bigg[& \frac{1}{\bar{k}^2 - M_t^{\star 2} + i\epsilon} \\ & + \frac{i\pi}{E_{\mathbf{k}}^\star} \delta(\bar{k}^0 - E_{\mathbf{k}}^\star) \theta(k_F - |\mathbf{k}|) \Bigg] \ , \end{aligned} \tag{23}$$

written in terms of the Fermi momentum (k_F). Note that we have also introduced effective masses and energies for the target nucleons

$$\begin{aligned} M_t^\star = M + \Sigma_{\rm s} \ ; \quad E_{\mathbf{k}}^\star = \sqrt{\mathbf{k}^2 + M_t^{\star 2}} \ ; \\ \bar{k}^\mu = (k^0 - \Sigma_{\rm v}, \mathbf{k}) \ . \end{aligned} \tag{24}$$

These are shifted from their free-space values by the scalar ($\Sigma_{\rm s}$) and vector ($\Sigma_{\rm v}$) mean fields, respectively. Also notice that since we are integrating over the four-momentum of the target nucleon the contribution from the (constant) vector potential can be eliminated by a simple change of variables. Formally, then, the response of the mean-field ground state is identical to the one of a relativistic Fermi gas. All vestige of the relativistic ground-state dynamics is subsumed into an effective nucleon mass.

The simplest model of the nuclear response that we will employ is a relativistic free Fermi gas. In this model the nuclear response consists of the excitation of particle-hole pairs subject to the constrains imposed by energy-momentum conservation and the Pauli exclusion principle. One can improve this description by taking into account, at least at the mean-field level, the interactions between the nucleons in the medium. This dressing leads to a shift in the nucleon mass but preserves the spectral content of the response. Note that since the nuclear response is being probed in the spacelike region ($q_\mu^2 < 0$) $N\bar{N}$ pairs cannot be excited in these models. They can, however, be virtually produced. Indeed, the virtual excitation of $N\bar{N}$ pairs is an important component of the RPA response. RPA correlations play a fundamental role in the behavior of isovector observables — particularly in R_L/R_T — and their inclusion is one of the central results from the present paper.

We now generalize the above expression for the scalar polarization to an arbitrary Lorentz structure

$$i\Pi_{ab}^{\alpha\beta}(q) = \int \frac{d^4k}{(2\pi)^4} {\rm Tr}\left[\lambda^\alpha \tau_a G(k+q) \lambda^\beta \tau_b G(k) \right] \ . \tag{25}$$

Note that the appropriate isospin matrices have been included to reflect the isovector character of the $(\vec{p},\vec{n})$ reaction. Many-body correlations are incorporated by considering the residual interaction between the particle and the hole. Formally, this is accomplished by solving Dyson's equation for the correlated RPA propagator [14]. The RPA equation is characterized by an infinite summation of the lowest-order (uncorrelated) polarization

$$\widetilde{\Pi}_{ab}^{\alpha\beta} = \Pi_{ab}^{\alpha\beta} + \Pi_{ac}^{\alpha 5} V_{cd}^{(\pi)} \Pi_{db}^{5\beta} + \Pi_{ac}^{\alpha\mu} V_{\mu\nu;cd}^{(\rho)} \Pi_{db}^{\nu\beta} + \cdots \ . \tag{26}$$

Note that we have written the residual particle-hole interaction in terms of $\pi + \rho$ contributions (the issue of short-range correlations is postponed until the next section)

$$\begin{aligned} V_{ab}^{(\pi)}(q) &= \delta_{ab} V^{(\pi)}(q) = \delta_{ab} f_\pi^2 \Delta(q) = \delta_{ab} \frac{f_\pi^2}{q_\mu^2 - m_\pi^2} \ , \\ V_{\mu\nu;ab}^{(\rho)}(q) &= \delta_{ab} V_{\mu\nu}^{(\rho)}(q) = \delta_{ab} g_\rho^2 D_{\mu\nu}(q) \\ &= \delta_{ab} \left[-g_{\mu\nu} + \frac{q_\mu q_\nu}{m_\rho^2} \right] \frac{g_\rho^2}{q_\mu^2 - m_\rho^2} \ . \end{aligned} \tag{27}$$

Because the ground state of nuclear matter is assumed to be isospin symmetric, and because both (π and ρ) propagators are diagonal in isospin, the isospin structure of the polarizations is simple and given by

$$\widetilde{\Pi}_{ab}^{\alpha\beta}(q) = \delta_{ab} \widetilde{\Pi}^{\alpha\beta}(q) \ ; \quad \Pi_{ab}^{\alpha\beta}(q) = \delta_{ab} \Pi^{\alpha\beta}(q) \ , \tag{28}$$

where the RPA polarizations satisfy

$$\widetilde{\Pi}^{\alpha\beta}(q) = \Pi^{\alpha\beta}(q) + \Pi^{\alpha i}(q) \widetilde{V}_{ij}(q) \Pi^{j\beta}(q) \ . \tag{29}$$

The RPA polarizations ($\widetilde{\Pi}$) have been written in terms of the lowest order polarizations and the medium-modified isovector interaction ($\widetilde{V}$). The latin indices i and j, with values in the range $-1, 0, 1, 2, 3$, are used to denote the "elementary" coupling of the nucleon to, either,

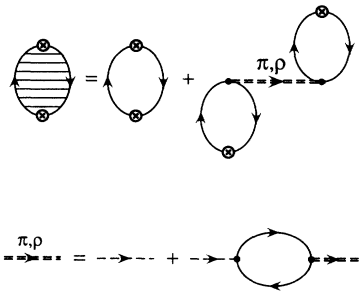

FIG. 1. Feynman diagrams representing the RPA polarizations [Eq. (29)] and Dyson's equation for the isovector interaction [Eq. (30)].

the $\pi(i=-1)$ or the $\rho(i=0,1,2,3)$ mesons (this coupling is represented by a dot in Fig. 1). In contrast, the greek indices α and β represent, as before, any of the five Lorentz structures (S,V,T,P,A) present in the NN amplitude (we have represented this coupling by a cross in Fig. 1). The RPA dynamics is, thus, fully contained in the medium-modified isovector interaction satisfying the following Dyson's equation:

$$\widetilde{V}_{ij}(q) = V_{ij}(q) + V_{ik}(q)\Pi^{kl}(q)\widetilde{V}_{lj}(q) \ . \tag{30}$$

Note that the free-space interaction V_{ij} is diagonal

$$V_{ij} = \begin{pmatrix} V^{(\pi)} & 0 \\ 0 & V^{(\rho)}_{\mu\nu} \end{pmatrix} \ , \tag{31}$$

and that the elementary NN-meson vertex (denoted by Λ^i in the next section) will be dictated by our choice of residual particle-hole interaction.

C. Residual particle-hole interaction: $\pi + \rho + g'$

The residual interaction consists of $\pi+\rho+g'$ contributions. For the $NN\pi$ coupling we assume a pseudovector representation. It is convenient to adopt this, as opposed to a pseudoscalar, representation because it incorporates the correct low-energy pion dynamics without sensitive cancellations [10]. The ρ meson contains a vector as well as a tensor coupling to the nucleon. With these choices we have specified completely the elementary $NN\pi$ and $NN\rho$ vertices to be used in Eqs. (29) and (30):

$$\Lambda^i = \begin{cases} \dfrac{\not{q}}{m_\pi}\gamma^5 & \text{if } i=\pi; \\ \left(\gamma^\mu \pm iC_\rho\sigma_{\mu\nu}\dfrac{q_\nu}{2M}\right) & \text{if } i=\rho. \end{cases} \tag{32}$$

Note that the plus (minus) sign should be used when the four-momentum of the ρ meson flows into (away from) the vertex (in the case of the pion the minus sign has been incorporated into the definition of $V^{(\pi)}$). The π and ρ components of the NN potential in the nonrelativistic limit are well known. The one-pion-exchange contribution is given by

$$V_\pi(\mathbf{q}) = -\frac{f_\pi^2}{m_\pi^2}\frac{(\sigma_1\cdot\mathbf{q})(\sigma_2\cdot\mathbf{q})}{\mathbf{q}^2+m_\pi^2}(\tau_1\cdot\tau_2) \ , \tag{33}$$

where the "spin-longitudinal" coupling

$$\frac{f_\pi^2}{4\pi} = \left(\frac{m_\pi}{2M}\right)^2\frac{g_\pi^2}{4\pi} \tag{34}$$

has been defined in terms of the couplings and masses listed in Table I [15]. Although the ρ meson contains a vector as well as a tensor coupling to the nucleon, the $NN\rho$ coupling is dominated by the large tensor contribution which, in particular, is responsible for generating the transverse character of the interaction

$$V_\rho(\mathbf{q}) = -\frac{f_\rho^2}{m_\rho^2}\frac{(\sigma_1\times\mathbf{q})\cdot(\sigma_2\times\mathbf{q})}{\mathbf{q}^2+m_\rho^2}(\tau_1\cdot\tau_2) \ . \tag{35}$$

Note that we have introduced the "spin-transverse" coupling

$$\frac{f_\rho^2}{4\pi} = \left(\frac{m_\rho}{2M}\right)^2\frac{g_\rho^2}{4\pi}C_\rho^2 \ , \tag{36}$$

in terms of the (large) tensor-to-vector ratio C_ρ. As it stands, the interaction is extremely attractive in the spin-spin channel. In order to regularize the large spin-spin component of the interaction one simulates the effect from repulsive short-range correlations by introducing a phenomenological Landau-Migdal parameter g'

$$V_{g'}(\mathbf{q}) = \frac{f_\pi^2}{m_\pi^2}g'(\sigma_1\cdot\sigma_2)(\tau_1\cdot\tau_2) \ . \tag{37}$$

The effect of g' will be incorporated by modifying, separately, the π and (the transverse component of) the ρ propagators. This can be accomplished with the use of the following identity:

$$(\sigma_1\cdot\sigma_2) = \Big[(\sigma_1\cdot\mathbf{q})(\sigma_2\cdot\mathbf{q}) + (\sigma_1\times\mathbf{q})\cdot(\sigma_2\times\mathbf{q})\Big] \ . \tag{38}$$

In this way, the spin-longitudinal and spin-transverse components of $V_{g'}$ get absorbed into redefinitions of "effective" π and ρ propagators

TABLE I. Meson masses, coupling constants, tensor-to-vector ratio, and Landau-Migdal parameter g' for the isovector interaction. The value of g' enclosed (not enclosed) in parentheses should be used when $M^\star \neq M$ ($M^\star = M$). Coupling constants have been adopted from Ref. [15].

Meson	Mass (MeV)	$g^2/4\pi$	$C=f/g$	g'
π	139	14.08	—	0.70 (0.70)
ρ	770	0.41	6.1	0.65 (0.30)

$$\Delta_\pi(q_\mu^2) = \frac{1}{q_\mu^2 - m_\pi^2} \to \left[\frac{1}{q_\mu^2 - m_\pi^2} - \frac{g'_\pi}{q_\mu^2}\right], \quad (39)$$

$$\Delta_\rho(q_\mu^2) = \frac{1}{q_\mu^2 - m_\rho^2} \to \left[\frac{1}{q_\mu^2 - m_\rho^2} - \frac{g'_\rho}{q_\mu^2}\right],$$

where

$$g'_\pi \equiv g' \; ; \quad g'_\rho \equiv g' \left[\left(f_\pi^2/m_\pi^2\right) \Big/ \left(f_\rho^2/m_\rho^2\right)\right] . \quad (40)$$

Thus effective, rather than free, π and ρ propagators are used in Eq. (27) to compute the residual isovector interaction. In all that follows we will assume the "standard" value of $g' = 0.7$ for the phenomenological Landau-Migdal parameter. Note that in this case $g'_\pi = 0.7$ and $g'_\rho \sim 0.65$ for the parameters given in Table I. We have displayed the resulting isovector interaction, in the static ($\omega = 0$) limit, in Fig. 2.

We now examine isoscalar effects, from a reduced nucleon mass in the medium, on the isovector response. At the simplest level a reduction in the value of the nucleon mass leads to a shift in the position and to an increase in the width of the quasielastic peak, i.e.,

$$\omega_{QE} = \frac{Q^2}{2M} \to \frac{Q^2}{2M^\star} \; ; \quad \Delta\omega \simeq \frac{qk_F}{M} \to \frac{qk_F}{M^\star} . \quad (41)$$

This simple realization, however, has nontrivial consequences for the case of the transverse response. Relative to a free Fermi-gas calculation the transverse response measured in quasielastic electron scattering appears to be quenched and hardened. This observation provides strong evidence in favor of strong repulsive correlations in the transverse spin-isospin channel. Note, however, that the uncorrelated response of a relativistic mean-field ground state is already "hardened" relative to the Fermi-gas response. This is a simple consequence of the in-medium reduction of the nucleon mass. Moreover, the transverse (e, e') response is dominated by the large isovector anomalous moment of the nucleon. Thus, the integrated response is insensitive to a change in the value of the nucleon mass. Since the width increases as $M^\star$ is reduced, the distribution appears to be quenched relative to the Fermi-gas response. Hence, the uncorrelated response of a relativistic mean-field ground state accounts for most of the features — quenching and hardening — observed experimentally. Indeed, in Fig. 3 a comparison is made between relativistic mean-field calculations of the transverse response and experimental data for ^{40}Ca(e, e') at momentum transfers of $q = 410$ and $q = 550$ MeV [16]. The dotted line shows the results from a finite-nucleus calculation of the Hartree (uncorrelated) response. Good agreement with experiment is found for the low-energy side of the quasielastic peak. The underestimation of transverse strength on the high-energy side of the peak, believed to be dominated by isobar formation and meson-exchange currents, is a common shortcoming of most "one-nucleon" models. The fact that experiment shows no hardening of the transverse response relative to the Hartree predictions is one of the important results of this comparison.

In Fig. 3 we have also included relativistic calculation of the nuclear-matter response with (solid line) and without (dashed line) RPA correlations. Based on our finite-nucleus results we have adjusted the spin-transverse component of the Landau-Migdal parameter to minimize the effect from RPA correlations. This could be achieved by selecting g'_ρ in the range $g'_\rho \sim (0.3 - 0.4)$. This represents a substantial reduction from its conventional $M^\star = M$ value of $g'_\rho \sim 0.65$. We will use $g'_\rho \equiv 0.3$ for $M^\star \neq M$ and $g'_\rho \equiv 0.65$ for $M^\star = M$, in all that follows. In Fig. 4 we have displayed the residual isovector interaction for the relativistic $M^\star \neq M$ case. It is important to realize that the value of g'_ρ is regarded as a purely phenomenological parameter constrained by electron-scattering data.

The longitudinal component of the residual interaction is also sensitive to a reduced effective nucleon mass in the

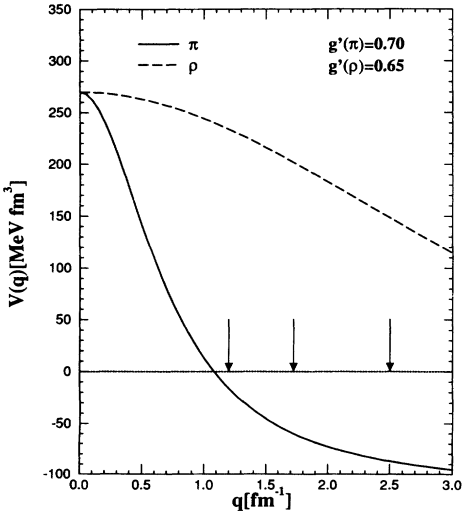

FIG. 2. Effective π and ρ contributions to the residual $M^\star = M$ interaction after the inclusion of the Landau-Migdal parameter. The static ($\omega = 0$) limit is assumed and the arrows are located at $q = 1.2, 1.72$, and 2.5 fm^{-1}.

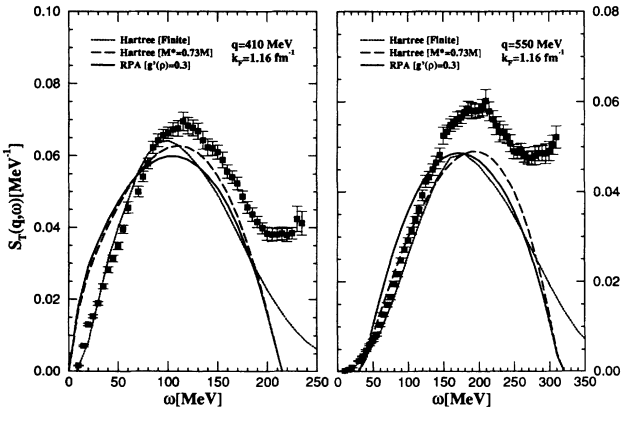

FIG. 3. Transverse response for ^{40}Ca(e, e') at $q = 410$ and 550 MeV. The dotted line is the Hartree response calculated in the finite nucleus. Nuclear-matter results with (solid line) and without (dashed line) RPA correlations are also displayed. The experimental data are from Ref. [16].

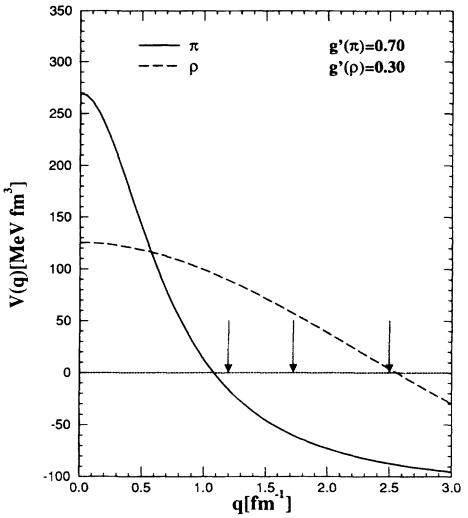

FIG. 4. Effective π and ρ contributions to the residual $M^\star \neq M$ interaction after the inclusion of the Landau-Migdal parameter. The static ($\omega = 0$) limit is assumed and the arrows are located at $q = 1.2, 1.72$, and 2.5 fm^{-1}.

medium. However, in contrast to the transverse component this modification does not emerge from a "phenomenological" tuning of parameters. Rather, it is a genuine dynamical effect that reduces the effective $NN\pi$ coupling in the medium. The origin of this reduction is as follows. In the medium, the pion-mediated NN interaction is given, according to Eq. (30), by

$$\widetilde{V}^{(\pi)}(q) = \epsilon_\pi^{-1}(q;k_F)V^{(\pi)}(q)\,, \qquad (42)$$
$$\epsilon_\pi(q;k_F) \equiv 1 - V^{(\pi)}(q)\Pi^{\rm PV}(q)\,,$$

where we have introduced the pion dimesic function ϵ_π and have defined the pseudovector polarization by [11]

$$i\Pi^{\rm PV}(q) = \left(\frac{q_\mu}{m_\pi}\right)\left(\frac{q_\nu}{m_\pi}\right) \times \int \frac{d^4k}{(2\pi)^4}{\rm Tr}\left[\gamma^\mu\gamma^5 G(k+q)\gamma^\nu\gamma^5 G(k)\right]\,. \qquad (43)$$

In the absence of a mass term from Walecka's mean-field Lagrangian, the axial-vector current would be conserved and the pseudovector polarization would vanish. Thus, any finite contribution to $\Pi^{\rm PV}$ must arise — and be proportional to — the nucleon mass. Indeed, in a previous study we determined the following behavior for the pion dimesic function in the static limit:

$$\epsilon_\pi(|\mathbf{q}|;k_F) = 1 - \frac{\mathbf{q}^2}{\mathbf{q}^2+m_\pi^2} f_\pi^2 M^{\star 2}\frac{2}{\pi^2|\mathbf{q}|} \times \int_0^{k_F} dk\,\frac{k}{E_{\mathbf{k}}^\star}\ln\left|\frac{|\mathbf{q}|+2k}{|\mathbf{q}|-2k}\right|\,, \qquad (44)$$

which suggests the following limits for the effective $NN\pi$ coupling in the medium

$$\frac{f_\pi^{\star 2}}{f_\pi^2} = \begin{cases} \left(\frac{M^\star}{M}\right) & \text{at low density;} \\ \left(\frac{M^\star}{M}\right)^2 & \text{at high density.} \end{cases} \qquad (45)$$

Note that the effective coupling is strongly density dependent. Indeed, the suppression of the effective $NN\pi$ coupling with increasing density more than compensates for the increase in the value of the integral leading, in particular, to no pion condensation — even in the absence of a phenomenological Landau-Migdal parameter ($g' \equiv 0$) [11]. This dynamical suppression of the $NN\pi$ coupling in the medium is instrumental in reducing the enhancement of the longitudinal spin response relative to nonrelativistic ($M^\star = M$) predictions [8].

D. Spin-transfer observables

Spin-transfer observables for the $(\vec{p},\vec{n})$ [and also for the $(\vec{p},\vec{p}')$] reaction can be obtained as linear combinations of the spin-dependent cross sections defined in Eq. (16). In particular, the out-of-plane observables ($\mathbf{s} = \mathbf{s}' = \hat{\mathbf{n}}$) are given by

$$\sigma = \left(\sigma_{++} + \sigma_{+-} + \sigma_{-+} + \sigma_{--}\right)\,, \qquad (46)$$
$$\sigma P = \left(\sigma_{++} + \sigma_{+-} - \sigma_{-+} - \sigma_{--}\right)\,, \qquad (47)$$
$$\sigma A_y = \left(\sigma_{++} - \sigma_{+-} + \sigma_{-+} - \sigma_{--}\right)\,, \qquad (48)$$
$$\sigma D_{NN} = \left(\sigma_{++} - \sigma_{+-} - \sigma_{-+} + \sigma_{--}\right)\,, \qquad (49)$$

where we have introduced the following simplified notation:

$$\frac{d^2\sigma_{\pm\hat{n}\pm\hat{n}}}{d\Omega dE'} \equiv \sigma_{\pm\pm}\,.$$

Since the conservation of parity forces sideways and longitudinal polarizations and analyzing powers to vanish, the remaining four independent observables, namely, $D_{S'S}, D_{L'S}, D_{S'L}$, and $D_{L'L}$, can all be obtained from the in-plane cross sections in analogy to D_{NN}.

The simplicity of the reaction mechanism (i.e., quasifree knockout) in quasielastic $(\vec{p},\vec{n})$ scattering makes the study of the nuclear spin-isospin response particularly clean. That the dominant mechanism in the reaction is, indeed, quasifree knockout can be justified by studying certain combinations of spin observables. Specifically, we consider $(P - A_y)$ and $[(D_{S'L} + D_{L'S}) - (D_{L'L} + D_{S'S})\tan(\theta_{\rm lab})]$. Due to time-reversal invariance these combinations are identically zero in elastic scattering and have been plotted in Fig. 5 for ^{40}Ca$(\vec{p},\vec{n})$ at $q = 1.72$ fm^{-1}. The fact that both of these observables are consistent with zero all across the quasielastic region is strong evidence in support of a quasifree mechanism for the reaction.

One of the most appealing features of having a complete set of spin-transfer observables is the possibility of extracting nuclear response functions, such as the spin-longitudinal response, which are not accessible with electromagnetic probes. Under certain approximations,

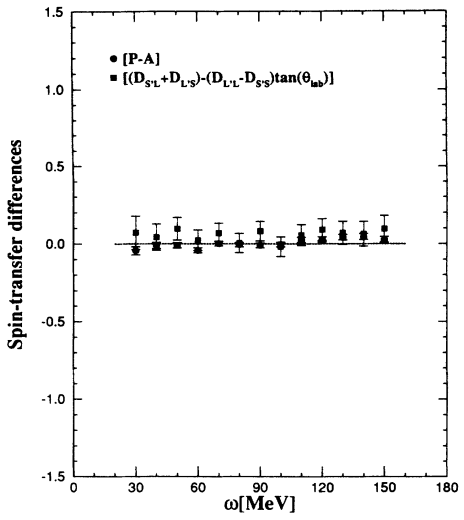

FIG. 5. Spin-transfer combinations $(P - A_y)$ and $[(D_{S'L} + D_{L'S}) - (D_{L'L} + D_{S'S})\tan(\theta_{\rm lab})]$ for ^{40}Ca$(\vec{p},\vec{n})$ at $q = 1.72$ fm^{-1}. Both combinations vanish in elastic scattering. The experimental data are from Ref. [4].

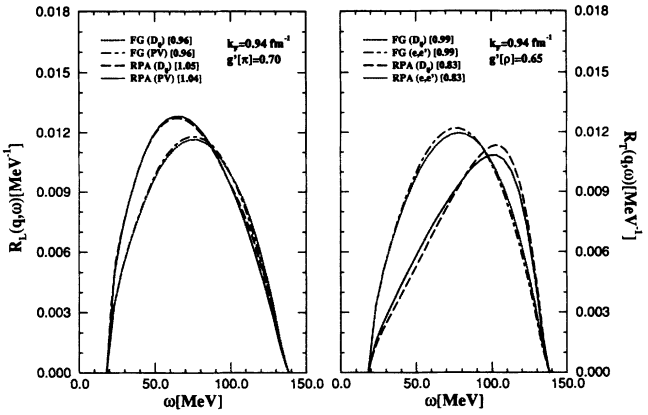

FIG. 6. Spin-longitudinal and spin-transverse response functions calculated from nuclear matter with and without the inclusion of RPA correlations. The response functions were either reconstructed from the spin-transfer observables or directly computed from appropriate polarization insertions. The quantities in square brackets give the value of the integrated response.

these responses can be directly related to linear combinations of the standard spin-transfer coefficients [1,17,18]

$$D_0 = \frac{1}{4}[(1 + D_{NN}) + (D_{S'S} + D_{L'L})\cos(\bar{\theta}) - (D_{S'L} - D_{L'S})\sin(\bar{\theta})] , \quad (50)$$

$$D_N = \frac{1}{4}[(1 + D_{NN}) - (D_{S'S} + D_{L'L})\cos(\bar{\theta}) + (D_{S'L} - D_{L'S})\sin(\bar{\theta})] , \quad (51)$$

$$D_L = \frac{1}{4}[(1 - D_{NN}) + (D_{S'S} - D_{L'L})\sec(\theta_{\rm lab})] , \quad (52)$$

$$D_T = \frac{1}{4}[(1 - D_{NN}) - (D_{S'S} - D_{L'L})\sec(\theta_{\rm lab})] , \quad (53)$$

where we have defined $\bar{\theta} \equiv \theta_{\rm c.m.} - \theta_{\rm lab}$. Note, in particular, that this new set of polarization-transfer observables satisfy the constraint

$$D_0 + D_N + D_L + D_T = 1 . \quad (54)$$

Nuclear responses per target nucleon, $R_i(\mathbf{q},\omega)$, can now be defined according to

$$R_i(\mathbf{q},\omega)A_{\rm eff} \equiv \left[\frac{1}{\sigma_{NN}}\left(\frac{d^2\sigma}{d\Omega dE'}\right)\right]\left[\frac{(D_i)_{NA}}{(D_i)_{NN}}\right] , \quad (55)$$

where $A_{\rm eff}$ represents the effective number of nucleons participating in the reaction.

Before proceeding further we show evidence in support of the above definition of the response. In Fig. 6 we have calculated spin-longitudinal and spin-transverse responses from nuclear matter using two different procedures. In one of them, the responses are reconstructed from the spin-transfer observables as outlined above. In the second method the responses are computed by assuming that only a pion (for R_L) or a ρ meson (for R_T) couple to the target nucleons. Thus, for R_L we compute the response directly from the pseudovector polarization given in Eq. (43). For the transverse response we simply report the electron-scattering result since it is known to be dominated by the anomalous (isovector-tensor) moment of the nucleon. The agreement between the two procedures, for both Fermi-gas and RPA responses, lends credibility to the approach. In particular we note, as previously advertised, that the longitudinal response becomes softened and enhanced, while the transverse hardened and quenched, relative to Fermi-gas predictions. We now examine how relativistic effects, mainly from a reduced nucleon mass, modify these findings.

III. RESULTS

We now proceed to show RPWIA results for all spin-transfer observables. Results will be presented using four different approximations. The simplest approximation consists of treating the nucleus as a relativistic free Fermi gas. In this case the various nuclear responses arise from imposing simple constraints such as energy-momentum conservation and the Pauli principle. Thus, no important deviations in the values of spin observables are expected, since neither the underlying NN interaction nor the collective response of the target are modified. Next we consider the uncorrelated response of a relativistic Hartree ground state. In this case the propagation of a nucleon through the medium is modified by its interaction with the mean field. This results in a reduction of the nucleon mass which now modifies the underlying NN interaction since matrix elements of the amplitude are being computed with in-medium (as opposed to free) spinors. The last two approximations are obtained from the previous two by incorporating RPA correlations into

TABLE II. Average Fermi momenta and effective nucleon masses for an incident energy of $T_{\rm lab} = 495$ MeV. Parameters have been adopted from Ref. [6].

Target	k_F (fm^{-1})	M_p^*/M	M_t^*/M
^{12}C	0.91	0.91	0.87
^{40}Ca	0.94	0.90	0.85

the nuclear response. In both cases the longitudinal component of the residual interaction is the same while the transverse component is constrained by the transverse response measured in quasielastic electron scattering, as previously discussed. Relevant parameters characterizing the residual interaction and the effective nucleon masses are given in Tables I and II, respectively. Finally, we have used the FA90 phase-shift solution of Arndt [19] to generate the relativistic parametrization of the NN amplitude.

In Figs. 7 and 8 the complete set of spin observables at $q = 1.72$ fm^{-1} is compared to the experimental data. The differential cross section has been divided by the single-nucleon value and reported as a spin-averaged response

$$R(\mathbf{q},\omega) = \left[\frac{1}{\sigma_{NN}}\left(\frac{d^2\sigma}{d\Omega dE'}\right)\right] . \tag{56}$$

The experimental value for the single-nucleon cross section was obtained by integrating the strength under the quasifree peak for the ^{2}H$(\vec{p},\vec{n})$ reaction and was reported to be 11.5 mb/sr [4]. This agrees well with the free value of 11.6 mb/sr [19] and also with our own value of 11.4 mb/sr obtained from a "nuclear-matter" calculation in the limit of $k_F \to 0$. Note that we have divided our theoretical cross sections by 10.9 mb/sr which is the appropriate value at fixed $q = 1.72$ fm^{-1} (as opposed to fixed angle). Finally, we have adopted the value of $A_{\rm eff} = 6$ for the effective number of nucleons participating in the reaction and have shifted all observables by the reaction Q value assumed to be $Q = 18.1$ MeV [6].

The Fermi-gas response (dotted line) peaks at an energy loss corresponding to free NN scattering, namely, $\omega_{QE} \simeq (\sqrt{\mathbf{q}^2 + M^2} - M) + Q \simeq 77$ MeV. Moreover, the integrated Fermi-gas strength equals 5.9. We attribute the small difference between this value and $A_{\rm eff}$ to Pauli blocking. Since the momentum transfer ($q = 1.72$ fm^{-1}) is slightly smaller than twice the Fermi momentum ($2k_F = 1.88$ fm^{-1}) a few transitions are Pauli blocked as is evident in the behavior of the response on the low-ω side of the peak. Thus, aside from a small correction due to Pauli blocking, the Fermi-gas response consists of a simple redistribution of single-particle strength.

The Hartree ($M^\star \neq M$) response is depicted by the dot-dashed line (almost indistinguishable from the solid line). The shift in the position, and the increase in the width, of the quasielastic peak relative to the Fermi-gas response are clearly evident and supported by experiment. Note, however, that the strength under the Hartree peak amounts to only 4.9. This reduction, which now underestimates the data, is caused by a modification of the effective NN interaction in the medium since $\bar{U}(M^\star)\not{q}\gamma^5 U(M^\star)$ is less than $\bar{U}(M)\not{q}\gamma^5 U(M)$.

The RPA response of the Fermi-gas ground state (dashed line) is hardened and quenched relative to the Fermi-gas response. Note that the integrated RPA strength is 5.5. This suggests that, at least for the spin-averaged response, the repulsive character of the transverse interaction dominates over the attractive longitudinal component (see Fig. 2). In contrast, RPA correlations have no observable effect on the $M^\star \neq M$ spin-averaged response (solid line). At this momentum transfer, the weaker repulsion from the transverse channel is almost completely canceled by the longitudinal attraction (see

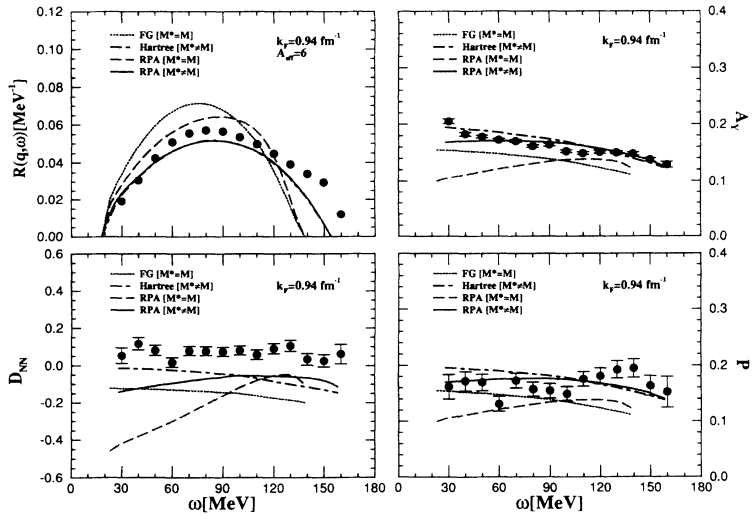

FIG. 7. Cross section (divided by its single-nucleon value), and out-of-plane spin observables for ^{40}Ca$(\vec{p},\vec{n})$ at $q = 1.72$ fm^{-1}. The dotted (dashed) line displays the uncorrelated (RPA) Fermi-gas result. The dot-dashed (solid) line gives the uncorrelated (RPA) result using medium-modified nucleon masses. The experimental data are from Ref. [4].

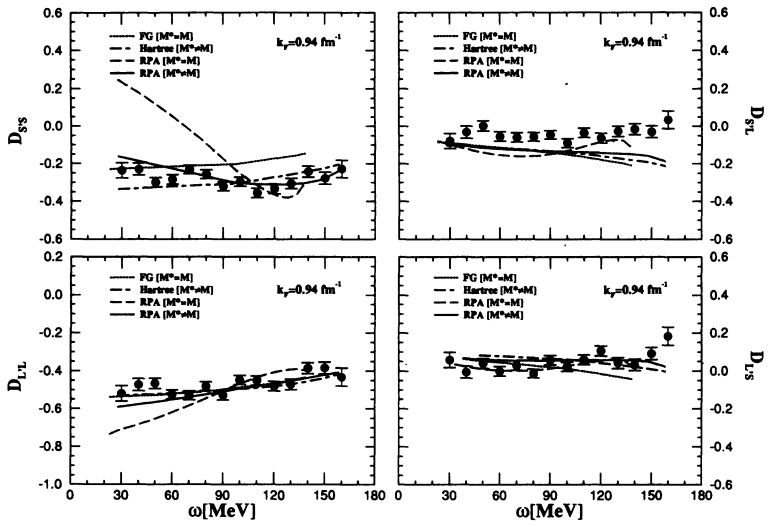

FIG. 8. In-plane spin-transfer observables for ^{40}Ca$(\vec{p},\vec{n})$ at $q = 1.72$ fm^{-1}. The dotted (dashed) line displays the uncorrelated (RPA) Fermi-gas result. The dot-dashed (solid) line gives the uncorrelated (RPA) result using medium-modified nucleon masses. The experimental data are from Ref. [4].

Fig. 4) resulting in an integrated response of 4.9, as in the Hartree case.

As for the remaiming spin observables, some systematic trends emerge. First, RPA correlations with free masses (dashed lines) generate dramatic changes with respect to the Fermi-gas values (dotted lines) and give a poor description of the data. In contrast, relativistic ($M^\star \neq M$) RPA correlations (solid lines) lead to a good description of the data and, in all cases, to an improvement over the Fermi-gas predictions. Perhaps the only case in which the agreement is not as good is for D_{NN}. Notice, however, that this discrepancy is present even at the level of the free NN observables (see Table III). This suggests that a more faithful representation of the many-body dynamics could be obtained by removing the "single-nucleon" component of the observable, as was done for the cross section.

In Fig. 9 we have plotted the new set of polarization-transfer observables relative to their free NN values. The fact that the spin-independent component D_0 is ill determined is a reflection of the spin-dependent character of the $(\vec{p},\vec{n})$ reaction. This, however, does not pose any serious limitation on the analysis since only three of the four observables are known to be independent [see Eq. (54)]. The data show, if at all, very small deviations from unity. The Fermi gas (dotted line), and to a lesser extent the Hartree (dot-dashed line), results are also close to unity but, arguably, the best overall description of the data is obtained with the relativistic RPA calculation (solid line). Instead, a poor description of the experimental observables is obtained whenever RPA correlations with free nucleon masses are included (dashed line). Yet, these results conform to the notion of a hardened transverse (D_N and D_T) and a softened longitudinal (D_L) response. Note that the actual responses are obtained from the above observables by multiplying them by the spin-averaged response $R(\mathbf{q},\omega)$ (see Fig. 7). Perhaps the most prominent feature of our results is the mild enhancement predicted for D_L by the relativistic RPA calculation (solid line). This behavior is a direct consequence of the dynamical suppression of the $NN\pi$ coupling in the medium, as discussed in Sec. II C.

The spin-longitudinal to spin-transverse ratio, R_L/R_T, is shown in Fig. 10. This plot summarizes — and dramatizes — some of the findings of the previous plot. Fermi-gas predictions (dotted line) are seen to be consistent with unity while Hartree results (dot-dashed line) show a mild suppression arising from a modified NN interaction in the medium. RPA correlations with free nucleon masses (dashed line) suggest a large enhancement in the ratio which is not observed experimentally and is reminiscent of the original nonrelativistic predictions. Finally, dynamical effects from a reduced nucleon mass in the medium generate a large suppression in the ratio (solid line) relative to the $M^\star = M$ predictions, in good agreement with experiment.

One important test for all models of the $(\vec{p},\vec{n})$ reaction is the momentum-transfer dependence of the ratio. This is so because competing models predict a different behavior with momentum transfer of the residual interaction. Specifically, a residual interaction having a transverse component modified by an in-medium reduction of the ρ meson mass [20] gives a description of R_L/R_T at $q \simeq 1.72$ fm^{-1} of similar quality to the relativistic case [21]. Yet, these two models predict a vastly different momentum-transfer dependence for the ratio. In partic-

TABLE III. Spin-transfer observables from the ^{2}H$(\vec{p},\vec{n})$ reaction at $q = 1.72$ fm^{-1} compared to the free NN values (obtained from the nuclear-matter calculation in the $k_F \to 0$ limit).

A_y	P	D_{NN}	$D_{S'S}$	$D_{S'L}$	$D_{L'S}$	$D_{L'L}$
0.13 ± 0.00	0.12 ± 0.01	0.01 ± 0.03	-0.21 ± 0.03	-0.11 ± 0.03	-0.03 ± 0.03	-0.47 ± 0.03
0.14	0.14	−0.15	−0.20	−0.14	0.03	−0.52

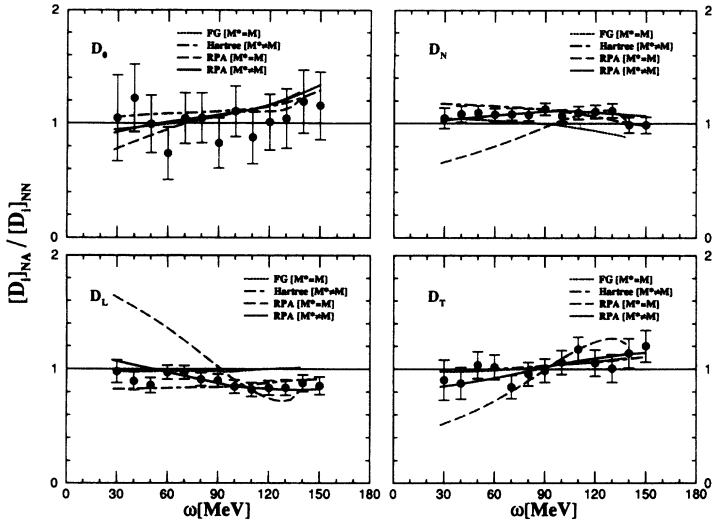

FIG. 9. Polarization-transfer observables divided by their single-nucleon value for $^{40}\mathrm{Ca}(\vec{p},\vec{n})$ at $q = 1.72$ fm^{-1}. The dotted (dashed) line displays the uncorrelated (RPA) Fermi-gas result. The dot-dashed (solid) line gives the uncorrelated (RPA) result using medium-modified nucleon masses. The experimental data are from Ref. [4].

ular, a reduced ρ-meson mass generates an enhancement — rather than a quenching — in R_L/R_T at $q \simeq 2.5$ fm^{-1}. This arises from a transverse component that has become attractive at $q \gtrsim 2.2$ fm^{-1} due to a faster falloff induced by the in-medium reduction of the ρ-meson mass. In contrast, in the relativistic model the qualitative features of the isovector interaction, namely, attractive longitudinal and repulsive transverse components, remain unchanged over the entire range of momentum transfers sampled in the experiment [22]. Note, these two models also make definite, and most likely different, predictions for the momentum-transfer dependence of the transverse response measured in inclusive electron scattering.

In Fig. 11 we display the relativistic predictions for the momentum-transfer dependence of R_L/R_T in ^{12}C.

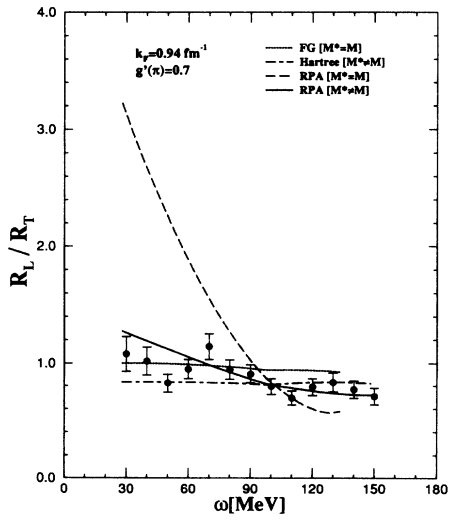

FIG. 10. Spin-longitudinal to spin-transverse ratio for $^{40}\mathrm{Ca}(\vec{p},\vec{n})$ at $q = 1.72$ fm^{-1}. The dotted (dashed) line displays the uncorrelated (RPA) Fermi-gas result. The dot-dashed (solid) line gives the uncorrelated (RPA) result using medium-modified nucleon masses. The experimental data are from Ref. [4].

Since the A dependence of the spin observables is known to be weak, the good agreement between theory and experiment at $q = 1.72$ fm^{-1} is not surprising. One also observes that the trends inferred from the $q = 1.72$ fm^{-1} calculations are preserved at low-momentum transfer, namely, a Fermi-gas value close to unity (dotted line), a slight suppression in the Hartree result (dot-dashed line), and a mild enhancement at low ω in the RPA value (solid line) which, however, now underestimates the experimental ratio (note, for a preliminary experimental report see Ref. [22]). In the absence of high-q data one could resolve this small discrepancy with a fine tuning of parameters.

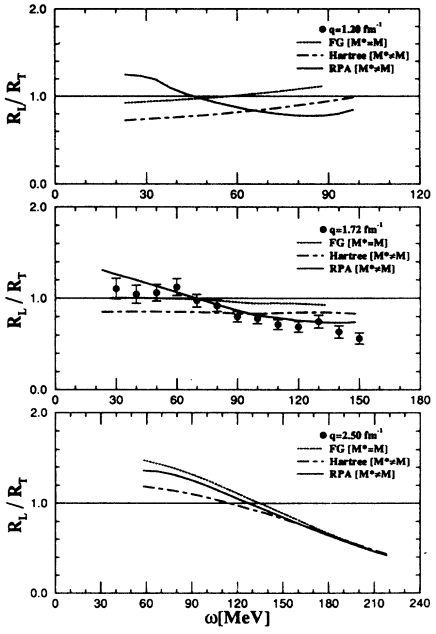

FIG. 11. Spin-longitudinal to spin-transverse ratio for $^{12}\mathrm{C}(\vec{p},\vec{n})$ at $q = 1.2, 1.72, 2.5$ fm^{-1}. The dotted line displays the Fermi-gas result. The dot-dashed (solid) line gives the uncorrelated (RPA) result using medium-modified nucleon masses. The experimental data are from Ref. [4].

Indeed, a slight increase in g'_ρ, or, alternatively, a slight decrease in g'_π, could enhance the ratio at low ω and, thus, bring the calculations into agreement with experiment. Explaining the reported quenching of R_L/R_T at $q = 2.5$ fm^{-1} [22], however, is likely to require physics that is absent from our model. Note that at $q = 2.5$ fm^{-1} even the Fermi-gas (dotted line) and Hartree (dot-dashed line) ratios are already enhanced at low ω relative to the free NN ratio. Moreover, since the transverse component of the interaction is never as attractive as the longitudinal one (at least within the range plotted in Fig. 4) the RPA ratio will exceed the Hartree value — and, thus, unity — at all values of q.

Some insight into the missing physics can be obtained from the distorted-wave calculations of Ichimura and collaborators. For the original $q = 1.72$ fm^{-1} calculation, it was shown that while distortions provide an overall reduction of the cross section, they do so without substantially modifying the distribution of strength [7]. Recently, however, they have suggested that distortions play a significant role in R_L/R_T at both $q = 1.2$ fm^{-1} and $q = 2.5$ fm^{-1} [22]. In particular, they found that, relative to the free NN values, distortions enhance the ratio at $q = 1.2$ fm^{-1}, but quench it at $q = 2.5$ fm^{-1}. Therefore, it is conceivable that after the inclusion of distortions, relativistic RPA calculations could yield a reasonable description of the experimental ratio for all three values of q. This expectation is currently under investigation.

IV. CONCLUSIONS

We have calculated all spin-transfer observables for the quasielastic $(\vec{p},\vec{n})$ reaction using a relativistic random-phase approximation to the Walecka model. Isoscalar effects arising from a dynamical reduction in the nucleon mass are responsible for a shift in the position and for an increase in the width of the quasielastic peak. These two features, by themselves and without RPA correlations, are sufficient to explain the quenching and hardening of the transverse response. Moreover, the reduced value of the nucleon mass generates a dynamical suppression of the $NN\pi$ coupling in the medium. This effect reduces the enhancement of the longitudinal response relative to an equivalent "nonrelativistic" ($M^\star \equiv M$) calculation. As a consequence, a good description of all spin-transfer observables is obtained at $q = 1.72$ fm^{-1}. In particular, we observed no enhancement in the spin-longitudinal to spin-transverse ratio, in agreement with experiment.

Brown and Wambach have offered an alternative explanation for the lack of an enhancement in R_L/R_T at $q = 1.72$ fm^{-1} by invoking a rescaling of the ρ-meson mass in the nuclear medium [21]. However, a recent report on the measurement of R_L/R_T at $q = 1.2$ fm^{-1} and $q = 2.5$ fm^{-1} suggests that the real picture might be more complicated than the one presented by either of these two models [22]. Particularly noteworthy are the results at $q = 2.5$ fm^{-1}. The experimental results seem to confirm the suppression at low-energy loss of R_L/R_T predicted by the $(m^\star_\rho)$ rescaling model. Yet, the data do not support the rapid variation with energy loss suggested by the model. Specifically, the rescaling model predicts $R_L/R_T \sim 1$ at the position of the quasielastic peak while the data remain constant at $R_L/R_T \sim 0.6$. For reference, the relativistic model overpredicts the ratio over the whole low-ω region of the quasielastic peak.

The distorted-wave calculations of Ichimura and collaborators might shed some light into the problem. We should note that these calculations do not incorporate any "novel" effect so they do overpredict the spin-longitudinal to spin-transverse ratio in RPA. Yet, their realistic treatment of distortions is very valuable. For example, these calculations revealed a modest effect of distortions on R_L/R_T at $q = 1.72$ fm^{-1} [7]. A recent report suggests, however, that distortions are important in enhancing and quenching the ratio at $q = 1.2$ fm^{-1} and $q = 2.5$ fm^{-1}, respectively [22]. Indeed, the distorted-wave calculations of Ichimura and collaborators — without RPA correlations — seem to be in good agreement with the experimental ratio at all three values of q. In particular, these trends suggest that relativistic RPA calculations with distortions could yield a good description of the momentum-transfer dependence of the ratio. It is clear, however, that before proceeding further with any theoretical comparison one must understand the interplay between "mundane" effects, such as distortions, and "novel" effects, such as meson-mass rescaling and/or relativity, in the determination of the isovector response.

There are, however, alternative ways of testing the different theoretical models. For example, one could concentrate on the individual spin-longitudinal and spin-transverse responses, rather than on their ratio. This has the advantage that the transverse response, even in plane wave, can be compared directly to electron-scattering data. Since in the rescaling model the transverse component of the interaction becomes attractive at $q \sim 2.2$ fm^{-1}, while it remains repulsive in the relativistic model, one could compare readily the (different) predictions of the two models with existing electron-scattering data [16].

Finally a word on future work. One of the early indications of a diminished role of isovector correlations in the medium came from the measurement of R_L/R_T in quasielastic $(\vec{p},\vec{p}')$ scattering [1,2]. Unfortunately, uncertainties associated with the removal of the isoscalar contribution clouded the interpretation. The $(\vec{p},\vec{n})$ reaction, on the other hand, is free from any isoscalar contamination and was advertised as the most promising method of observing the predicted enhancement of R_L/R_T. Thus, the advent of new experimental facilities and techniques opened the door to precision studies of the isovector response. Indirectly, these new facilities also opened the door to precision studies of the isoscalar response. Indeed, combined $(\vec{p},\vec{p}')$ and $(\vec{p},\vec{n})$ data — which now exist — should enable one, in principle, to extract the isoscalar spin-independent response R_0. This response is interesting because of its connection to the charge response measured in electron scattering and, thus, to the long-standing problem of the quenching of the Coulomb sum [16]. The charge response in electron scattering is dominated by the proton response which is half isoscalar and half isovector. Thus, electromagnetic probes are un-

able to isolate the pure isoscalar contribution to the response. Therein lies the appeal of the hadronic reactions.

Relativistic models of the electromagnetic response predict a substantial quenching of the charge response arising from isoscalar correlations [23]. Indeed, relativistic effects reduce the isoscalar charge response by as much as 50% relative to its Fermi-gas value. This large isoscalar quenching, however, is partially diluted by the isovector contribution to the electromagnetic response. Still, relativistic RPA results are about 25% below the Fermi-gas response and in good agreement with experiment. In the case of hadronic probes the surface-peaked nature of the reaction forces the probe to sample a lower-density region than in electron scattering and should suppress some of the large (~50%) isoscalar quenching. Still, a large reduction in R_0 appears to be an unavoidable consequence of the relativistic dynamics. A quantitative study of this effect is currently under investigation.

ACKNOWLEDGMENTS

We would like to thank X.Y. Chen and T.N. Taddeucci for making available the experimental data and for many helpful discussions. This research was supported by the Florida State University Supercomputer Computations Research Institute through the U.S. Department of Energy Contracts DE-FC05-85ER250000 and DE-FG05-92ER40750.

[1] T.A. Carey, K.W. Jones, J.B. McClelland, J.M. Moss, L.B. Rees, N. Tanaka, and A.D. Bacher, Phys. Rev. Lett. **53**, 144 (1984).
[2] L.B. Rees, J.M. Moss, T.A. Carey, K.W. Jones, J.B. McClelland, N. Tanaka, A.D. Bacher, and H. Esbensen, Phys. Rev. C **34**, 627 (1986).
[3] J.B. McClelland *et al.*, Phys. Rev. Lett. **69**, 582 (1992).
[4] X.Y. Chen *et al.*, Phys. Rev. C **47**, 2159 (1993).
[5] W.M. Alberico, M. Ericson, and A. Molinari, Nucl. Phys. **A379**, 429 (1982).
[6] C.J. Horowitz and D.P. Murdock, Phys. Rev. C **37**, 2032 (1988).
[7] M. Ichimura, in "Proceedings of the Fifth French-Japanese Symposium on Nuclear Physics," edited by K. Shimizu and O. Hashimoto (unpublished).
[8] C.J. Horowitz and J. Piekarewicz, Phys. Lett. B **301**, 321 (1993).
[9] J.D. Walecka, Ann. Phys. (N.Y.) **83**, 491 (1974).
[10] B.D. Serot and J.D. Walecka, in *Advances in Nuclear Physics*, edited by J.W. Negele and E. Vogt (Plenum, New York, 1986), Vol. 16.
[11] J.F. Dawson and J. Piekarewicz, Phys. Rev. C **43**, 2631 (1991).
[12] J.A. McNeil, L. Ray, and S.J. Wallace, Phys. Rev. C **27**, 2123 (1983).
[13] J.D. Bjorken and S.D. Drell, *Relativistic Quantum Fields* (McGraw-Hill, New York, 1965).
[14] A.L. Fetter and J.D. Walecka, *Quantum Theory of Many-Particle Systems* (McGraw-Hill, New York, 1971).
[15] R. Machleidt, K. Holinde, and Ch. Elster, Phys. Rep. **149**, 1 (1987); R. Machleidt, in *Proceedings of the Relativistic Dynamics and Quark-Nuclear Physics*, edited by M.B. Johnson and A. Picklesimer (Wiley, New York, 1986).
[16] P. Barreau *et al.*, Nucl. Phys. **A402**, 515 (1983).
[17] E. Bleszynski, M. Bleszynski, and C.A. Whitten, Jr., Phys. Rev. C **26**, 2063 (1982).
[18] C. Chan *et al.*, Nucl. Phys. **A510**, 713 (1990).
[19] R.A. Arndt and L. Roper, Scattering Analyses Interactive Dial-in program (SAID), Virginia Polytechnic Institute and State University (unpublished).
[20] G.E. Brown and M. Rho, Phys. Lett. B **237**, 3 (1990); Phys. Rev. Lett. **66**, 2720 (1991).
[21] G.E. Brown and J. Wambach, Nucl. Phys. **A568**, 895 (1994).
[22] T.N. Taddeucci, to appear in the Proceedings of the International Symposium on Spin-isospin Responses and Weak Processes in Hadrons and Nuclei, Osaka, Japan, 1994 (to be published).
[23] C.J. Horowitz and J. Piekarewicz, Phys. Rev. Lett. **62**, 391 (1989); Nucl. Phys. **A511**, 461 (1990).